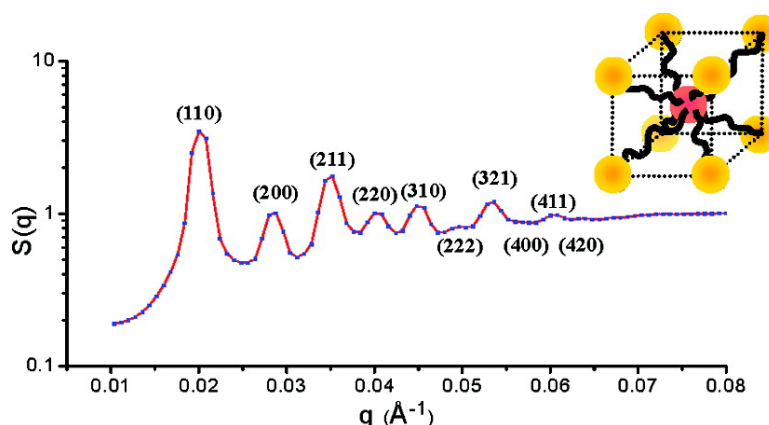


DNA Linker-Mediated Crystallization of Nanocolloids

Huiming Xiong, Daniel van der Lelie, and Oleg Gang

J. Am. Chem. Soc., **2008**, 130 (8), 2442-2443 • DOI: 10.1021/ja710710j

Downloaded from <http://pubs.acs.org> on February 8, 2009



More About This Article

Additional resources and features associated with this article are available within the HTML version:

- Supporting Information
- Links to the 1 articles that cite this article, as of the time of this article download
- Access to high resolution figures
- Links to articles and content related to this article
- Copyright permission to reproduce figures and/or text from this article

[View the Full Text HTML](#)

DNA Linker-Mediated Crystallization of Nanocolloids

Huiming Xiong,[†] Daniel van der Lelie,[‡] and Oleg Gang^{*†}Center for Functional Nanomaterials and Biology Department, Brookhaven National Laboratory,
Upton, New York 11973

Received November 29, 2007; E-mail: ogang@bnl.gov

Nanocolloids (NCs) offer a promising platform for the creation of new types of materials via the incorporation of their functionalities into well-defined structures. Among the rich phases of NC assemblies,¹ crystalline phases are of especial interest for the development of novel magnetic, photonic and plasmonic metamaterials.² The tunability of interaction potential, geometrical shape, core material, and surface chemistry of NCs provide unprecedented possibilities for designing such “artificial atoms”. Conventionally, various interactions such as van der Waals force, electrostatic interaction, and entropic effects have been used to tune the intercolloidal potential.³ Recently, a strategy based on DNA hybridization to link colloids has been demonstrated⁴ and was successfully applied in biological detection.⁵ Although theoretical work has predicted diverse phases of DNA/colloid hybrid systems, the phase behavior of such systems on the nanoscale has not been well explored, and the formation of crystalline phases still remains a challenge.⁶ In this Communication we report DNA linker-assisted formation of a three-dimensional crystalline ordered phase of DNA capped gold NCs (AuNCs), which occupy only ~3% by volume of the lattice, and demonstrate the correlation between DNA design and the kinetics of ordered phase formation.

Generally, two approaches are widely utilized for the assembly of DNA/NC hybrid systems: (i) direct hybridization of two types of complementary single-stranded (ss) DNAs tethered on NCs^{4a,d} and (ii) NC hybridization with linker DNAs, whose two ends are complementary to the respective mutually noncomplementary ssDNAs on NCs.^{4c,e,f} The second approach is particularly attractive because of its potential of building various architectures from a given set of NCs *via* different linker designs. Herein we report a systematic, structural study of NC assemblies with flexible ssDNA linkers of different lengths and fixed DNA recognition ends. We found that formation of crystalline organization is evidently favored for longer ssDNA linker.

A binary set of AuNCs with a diameter 11.5 ± 1.1 nm was generated by functionalizing colloids with either type A or B of noncomplementary ssDNA (A = 5'-ATTGGAAGTGGATAA-(T)₁₅-C₃H₆-SH; B = HS-C₆H₁₂-(T)₁₅-TAACCTAACCTTCAT-3') (see Supporting Information). The ssDNA contains a 15 base-pair (bp) outer recognition part and a 15 bp poly dT, which serves as a spacer separating the recognition sequence from the AuNC surface. The melting temperature of the 15 bp outer recognition dsDNA is about 60 °C as measured by UV-vis spectrophotometry.⁷ The ends of the linker *L_n* ssDNAs (5'-TTATCCACTTCCAAT-(T)_{*n*}-ATGAAGGTTAGGTTA-3') are complementary to the respective ends of ssDNAs on AuNCs and are separated by a central flexible poly dT fragment which contains *n* nucleotides, having a length of 0, 15, 30, or 70 bp (denoted accordingly as Sys-L0, Sys-L15, Sys-L30, and Sys-L70). Each system was formed by mixing an equal mole of the two types of ssDNAs capped AuNCs and a linker

ssDNA (DNA/particle mole ratio 36:1) in 0.3 M PBS buffer, after which the mixture was incubated at 65 °C for 10 min, followed by cooling to room temperature for ~2 h.

Temperature-dependent synchrotron small-angle X-ray scattering (SAXS) is utilized to characterize the structure of assembled aggregates. Figure 1 illustrates an evolution of structure factors *S*(*q*) extracted from SAXS patterns upon heating for the representative system Sys-L30. Scattering profiles are obtained by azimuthal integration of the powderlike scattering in the SAXS patterns. At room temperature, a phase showing relatively broad peaks is observed. No apparent changes of the *S*(*q*) shape and its peak positions are detected upon heating from the room temperature to 56 °C when a sudden development of the *S*(*q*) is observed. At this temperature, a well-defined crystalline order is manifested by an increased number of diffraction peaks in *S*(*q*) and their decreased widths. Analysis of the detected seven orders of Bragg's peaks positions reveals a ratio $q/q_1 = 1:2^{1/2}:3^{1/2}:4^{1/2}:5^{1/2}:6^{1/2}:7^{1/2}$, which corresponds to body-centered cubic (BCC) lattice with *Im*3*m* symmetry. The relative intensities of the diffraction peaks are also in accordance with the predictions for BCC lattice (Figure 1). The first peak thus arises from the diffraction of {110} planes. At 56 °C, the lattice constant of the unit cell (*a*) is ~39 nm and the nearest-neighbor distance *d_{nn}* is ~34 nm. Considering the size of AuNC, the surface-to-surface distance between the nearest-neighbor AuNCs is about 22 nm, which is nearly twice the diameter of AuNC and agrees with the estimated length of the DNA (Supporting Information). When heated to 59 °C, the diffraction peaks disappear, indicating crystal melting and only residual scattering remains which can be attributed to the presence of disordered AuNC clusters. Upon subsequent cooling the BCC structure is formed again at a temperature just below 59 °C and the *d_{nn}* progressively decreases to ~32 nm at room temperature, as illustrated in Figure 2a, indicating a lattice constant change by ~3% over the studied temperature range. Once formed, the BCC crystalline order can be preserved for at least 2 months (experimental interval) in the buffer solution at room temperature.

To understand the evolution of the assembly order, the correlation length ξ is plotted as a function of temperature in Figure 2b, where ξ is approximated as $\xi \approx 2\pi/\Delta q$ and Δq is a resolution corrected full-width-at-half-maximum (fwhm) of the first diffraction peak⁸ (see Supporting Information). All studied systems exhibit a low degree of order below 56 °C, with ξ ranging from ~100 to ~200 nm. Once the temperature reaches the transition regime within a narrow temperature range of a few degrees around 55 °C, an increase to the instrumental resolution limited ξ (~550 nm) or larger for Sys-L30 and Sys-L70 is instantly observed, corresponding to formation of a BCC structure. In contrast, for Sys-L0 and Sys-L15, practically no ξ increase is observed, indicating that no ordered crystalline structures are formed.

Order perfection during the heating process is common in molecular systems.⁹ In pure hard-sphere systems temperature does

[†] Center for Functional Nanomaterials.[‡] Biology Department.

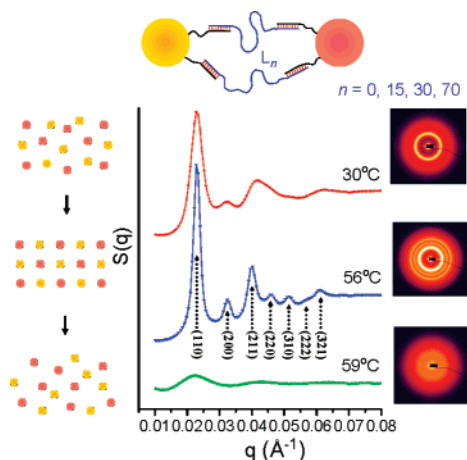


Figure 1. Schematic illustration and comprehensive temperature-dependent 2D SAXS patterns and respective extracted structure factors $S(q)$ of Sys-L30 during heating process.

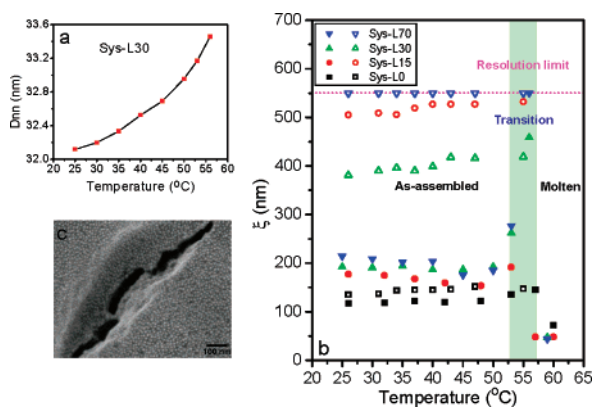


Figure 2. (a) Temperature dependent nearest-neighbor distance (d_{nn}) of Sys-L30 during cooling process (The line is only a guide for eyes); (b) temperature-dependent correlation lengths of $\{110\}$ planes of hybrid systems during heating process (filled symbols) and cooling process of corresponding annealed systems at 55 °C (open symbols); (c) SEM image of Sys-L30 colloidal crystals after dried in air.

not play an important role in phase behaviors, instead sphere volume fraction is the driving parameter.¹ However, in our systems where attraction is predominantly determined by DNA hybridization, the temperature increase allows gradual decreases of attraction strength. Specifically, when the system is brought close to its melting temperature, the reduced free energy of DNA hybridization results in a high probability of dynamically reforming DNA bridges. This allows local colloids rearrangement and the formation of close-to-equilibrium crystalline phases.

To study the effects of the DNA linker length on the formation of equilibrium crystalline phases, we allowed all the systems to anneal in transition regime at 55 °C for 2 h. As shown in Figure 2b, Sys-L70 with the longest linker is the most prone to order improvement during annealing. For Sys-L15, although there was little perfection during initial heating, the order increased tremendously after annealing. However, for Sys-L0 with no flexible part in the linker, the structure of NCs assembly remains disordered after the annealing process. Disordered aggregates are typically observed when the DNA linker is rigid.¹⁰ While high hybridization energy records the random way whenever nanocolloids collide, a rigid DNA may prohibit a local reconstruction of the newly formed structure. We presume that although the exact mechanism of crystal formation is not known, the flexibility of DNA linker is shown to

favor the ordering, while heating to premelting temperature provides a thermodynamic path from metastable state to crystalline phase.

In contrast with conventional hard sphere (or atomic) BCC crystal, in which the packing fraction is typically 68%, the volume occupancy of AuNCs in the unit cell is only 2–3%. The rest of the lattice is occupied by mobile solvent molecules and DNAs, which take another a few percentages. The DNA linkage between particles also leads to the high thermal expansion of the observed crystal phase, for example, ~3% for Sys-L30 (also see Table 1 in Supporting Information). Real space characterization of crystalline phase was conducted using scanning electron microscope (SEM), as shown in Figure 2c for dried Sys-L30 crystal, and reveals that the distance between colloidal surfaces is smaller than the 22 nm deduced from SAXS measurements. The high fraction of water in the lattice volume is thought to result in the structure's susceptibility to dryness and the crystalline order may not be preserved under SEM conditions.

In summary, we have demonstrated that crystallization of AuNCs can be achieved via hybridization of dispersed, mutually non-complementary ssDNA capped AuNCs with flexible ssDNA linker. The crystalline order formed close to the melting temperature in aqueous is preserved after cooling. The flexibility of the DNA linkage is found to play an important role in the formation of the BCC crystalline structure. The spatial openness of the observed structures may offer accommodation of additional functionalities. Phase behaviors and salts effects on molecular interactions and resulting structure are still to be explored.

Acknowledgment. Research was supported by the U.S. DOE Office of Science and Office of Basic Energy Sciences, under Contract No. DE-AC-02-98CH10886. We thank Y. Lin for the setup of NLS X21 beamline and A. Stein for the assistance with SEM. H.M.X. thanks M. M. Maye for help with AuNC synthesis and D. Nykypanchuk for SAXS instrumentation.

Supporting Information Available: Additional experimental details, SAXS, TEM, SEM, and DLS results. This material is available free of charge via the Internet at <http://pubs.acs.org>.

References

- (1) Russel, W. B.; Saville, D. A.; Schowalter, W. R. *Colloidal Dispersions*; Cambridge University Press: Cambridge, U.K., 1989.
- (2) (a) Smith, D. R.; Pendry, J. B.; Wiltshire, M. C. K. *Science* **2004**, *305*, 788–792. (b) Tao, A.; Sinsermsuksakul, P.; Yang, P. D. *Nat. Nanotechnol.* **2007**, *2*, 435–440.
- (3) Israelachvili, J. N. *Intermolecular and Surface Forces*; 2nd ed.; Academic Press: London, 1992.
- (4) (a) Mirkin, C. A.; Letsinger, R. L.; Mucic, R. C.; Storhoff, J. J. *Nature* **1996**, *382*, 607–609. (b) Alivisatos, A. P.; Johnson, K. P.; Peng, X. G.; Wilson, T. E.; Loweth, C. J.; Bruchez, M. P.; Schultz, P. G. *Nature* **1996**, *382*, 609–611. (c) Biancaneello, P. L.; Kim, A. J.; Crocker, J. C. *Phys. Rev. Lett.* **2005**, *94*, 058302. (d) Valignat, M. P.; Theodoly, O.; Crocker, J. C.; Russel, W. B.; Chaikin, P. M. *Proc. Natl. Acad. Sci. U.S.A.* **2005**, *102*, 4225–4229. (e) Nykypanchuk, D.; Maye, M. M.; van der Lelie, D.; Gang, O. *Langmuir* **2007**, *23*, 6305–6314. (f) Maye, M. M.; Nykypanchuk, D.; van der Lelie, D.; Gang, O. *Small* **2007**, *1678*–1682.
- (5) Rosi, N. L.; Mirkin, C. A. *Chem. Rev.* **2005**, *105*, 1547–1562.
- (6) Tkachenko, A. V. *Phys. Rev. Lett.* **2002**, *89*, 148303. (b) Lukatsky, D. B.; Frenkel, D. *Phys. Rev. Lett.* **2004**, *92*, 068302.
- (7) Maye, M. M.; Nykypanchuk, D.; van der Lelie, D.; Gang, O. *J. Am. Chem. Soc.* **2006**, *128*, 14020–14021.
- (8) Warren, B. E. *X-ray Diffraction*; Addison-Wesley Pub. Co.: Reading, MA, 1969.
- (9) (a) Cheng, S. Z. D.; Keller, A. *Ann. Rev. Mater. Sci.* **1998**, *28*, 533–562. (b) Wundlich, B. *Macromolecular Physics, Volume 2: Crystal Nucleation, Growth and Annealing*; Academic Press: New York, 1976.
- (10) (a) Park, S. J.; Lazarides, A. A.; Storhoff, J. J.; Pesce, L.; Mirkin, C. A. *J. Chem. Phys. B* **2004**, *108*, 12375–12380. (b) Storhoff, J. J.; Lazarides, A. A.; Mucic, R. C.; Mirkin, C. A.; Letsinger, R. L.; Schatz, G. C. *J. Am. Chem. Soc.* **2000**, *122*, 4640–4650.

JA710710J